THE JOURNAL OF BIOLOGICAL CHEMISTRY VOL. 282, NO. 31, pp. 22481–22491, August 3, 2007

Molecular and Biochemical Analysis of the Plastidic ADP-glucose Transporter (ZmBT1) from *Zea mays*[*] [S]

Received for publication, March 22, 2007, and in revised form, May 8, 2007 Published, JBC Papers in Press, June 11, 2007, DOI 10.1074/jbc.M702484200

Simon Kirchberger[‡], Michaela Leroch[‡], Martijn A. Huynen[§], Markus Wahl[‡], H. Ekkehard Neuhaus[‡], and Joachim Tjaden[‡1]

From the [‡]Abteilung Pflanzenphysiologie, Fachbereich Biologie, Technische Universität Kaiserslautern, P. O. Box 3049, D-67653 Kaiserslautern, Germany and the [§]Center for Molecular and Biomolecular Informatics, Nijmegen, and the Centre for Molecular Life Sciences, Radboud University, Nijmegen, Toernooiveld 1, NL-6525 ED Nijmegen, The Netherlands

Physiological studies on the *Brittle1* maize mutant have provided circumstantial evidence that ZmBT1 (*Zea mays* Brittle1 protein) is involved in the ADP-Glc transport into maize endosperm plastids, but up to now, no direct ADP-Glc transport mediated by ZmBT1 has ever been shown. The heterologous synthesis of ZmBT1 in *Escherichia coli* cells leads to the functional integration of ZmBT1 into the bacterial cytoplasmic membrane. ZmBT1 transports ADP-Glc in counterexchange with ADP with apparent affinities of about 850 and 465 μM, respectively. Recently, a complete ferredoxin/thioredoxin system has been identified in cereal amyloplasts and BT1 has been proposed as a potential Trx target protein (Balmer, Y., Vensel, W. H., Cai, N., Manieri, W., Schurmann, P., Hurkman, W. J., and Buchanan, B. B. (2006) *Proc. Natl. Acad. Sci. U. S. A.* 103, 2988–2993). Interestingly, we revealed that the transport activity of ZmBT1 is reversibly regulated by redox reagents such as diamide and dithiothreitol. The expression of Zm*BT1* is restricted to endosperm tissues during starch synthesis, whereas a recently identified *BT1* maize homologue, the Zm*BT1–2*, exhibits a ubiquitous expression pattern in hetero- and autotrophic tissues indicating different physiological roles for both maize BT1 isoforms. BT1 homologues are present in both mono- and dicotyledonous plants. Phylogenetic analyses classify the BT1 family into two phylogenetically and biochemically distinct groups. The first group comprises BT1 orthologues restricted to cereals where they mediate the ADP-Glc transport into cereal endosperm storage plastids during starch synthesis. The second group occurs in mono- and dicotyledonous plants and is most probably involved in the export of adenine nucleotides synthesized inside plastids.

Cereal crops accumulate starch in seed endosperm plastids as main energy reserve. The pathway of starch synthesis in cereal endosperms is unique and requires enzyme isoforms that are not present in other tissues or non-cereal plants. The ability of heterotrophic plastids to utilize cytosolic precursors to support their biosynthetic and catabolic pathways depends on the presence of specific transporters in the plastid envelope. In cereal endosperms, the ADP-glucose pyrophosphorylase (AGPase),[2] which catalyzes the first committed and rate-limiting step in starch biosynthesis, is mainly localized in the cytosol with a total AGPase activity of about 85–95% (2). Therefore, ADP-glucose (ADP-Glc) is synthesized in the cytosol of cereal endosperms as the main precursor for starch synthesis and has to be subsequently imported into the storage plastids.

Several maize (*Zea mays* L.) endosperm mutants affected in starch quality or quantity were used to elucidate critical steps in amyloplast starch synthesis. The *Waxy* gene, which encodes a starch-granule-bound starch synthase involved in amylose synthesis (3) and the *Shrunken-2* and *Brittle-2* genes, which encode subunits of the AGPase (4–6), were shown to be important for starch synthesis in maize. The *Brittle-1* (*BT1*) maize mutant was identified in 1926 (7, 8) and corresponding endosperm is severely reduced in starch content, which results in kernels with a collapsed angular appearance at maturity. The BT1 protein from *Z. mays* (ZmBT1) belongs to the mitochondrial carrier family and is located in the amyloplast envelope membrane (9, 10). The absence of ZmBT1 correlates with a 12-fold higher level of ADP-Glc in the cytosol of *BT1* mutant endosperm than in wild-type endosperm (11) and *BT1* mutant kernels accumulate about 80% less starch than wild-type kernels (12). The incorporation of externally applied ADP-Glc into starch in amyloplasts isolated from *BT1* mutant endosperm was reduced to about 25% compared with wild-type amyloplasts (13). These results indicate that ZmBT1 is involved in the transport of ADP-Glc into maize endosperm plastids (14), but up to now, no direct ADP-Glc transport mediated by ZmBT1 has been shown.

Recently, a BT1 homologue from a non-cereal plant, namely potato (StBT1 from *Solanum tuberosum*), was functionally characterized as a plastidic adenine nucleotide uniporter expressed in sink and source tissues (15). The physiological role of StBT1 is most likely the export of purine nucleotides that are exclusively *de novo* synthesized in plastids of autotrophic and heterotrophic tissues (15, 16). These novel findings further

* This work was supported by Deutsche Forschungsgemeinschaft Grant TJ 5/2-1 (to J. T.). The costs of publication of this article were defrayed in part by the payment of page charges. This article must therefore be hereby marked "*advertisement*" in accordance with 18 U.S.C. Section 1734 solely to indicate this fact.

[S] The on-line version of this article (available at http://www.jbc.org) contains supplemental Table S1 and Figs. S1–S4.

[1] To whom correspondence should be addressed: Technische Universität Kaiserslautern, Pflanzenphysiologie, Postfach 3049, D-67653 Kaiserslautern, Germany. Tel.: 0631-205-3040; Fax: 0631-205-2600; E-mail: tjaden@rhrk.uni-kl.de.

[2] The abbreviations used are: AGPase, ADP-glucose pyrophosphorylase; RT, reverse transcriptase; IPTG, isopropyl β-D-thiogalactopyranoside; EF, elongation factor; Trx, thioredoxin; DTT, dithiothreitol.

urged for a comprehensive analysis of the biochemical transport features of the maize homologue ZmBT1. We present here direct transport properties of the heterologously expressed ZmBT1. For this we exploited an *Escherichia coli* expression system that was successfully used to analyze plastidic or mitochondrial carrier proteins (15, 17, 18). We also reviewed the endosperm-specific expression of Zm*BT1* and proved the occurrence and expression pattern of further Zm*BT1* homologues in maize.

EXPERIMENTAL PROCEDURES

Cultivation of Plants—Maize plants (*Z. mays* L.) were grown in a greenhouse at 22–26 °C and watered once a day. The ambient light period was extended to 16 h/day with Philips Sont-Agro lights (200 μmol quanta m^{-2} s^{-1}). For RNA and genomic DNA isolation, maize tissues were collected and immediately frozen in liquid nitrogen until use.

Southern Blot Analyses—Genomic DNA was isolated from 4 g of frozen leaf tissue as described by Dellaporta *et al.* (19). About 10 μg of genomic DNA were digested with high concentrated restriction enzymes (BamHI, HindIII, XbaI, and XhoI). DNA fragments were separated in 0.8% agarose gels, denatured, and neutralized according to standard procedures (20). After transfer to nylon membranes (Hybond-N membranes, Amersham Biosciences), DNA fragments were fixed to the nylon filters by optimal UV cross-link (254 nm, 120 millijoule cm^{-2}) in a Spectrolinker. The membranes were prehybridized for 60 min at 68 °C in 6× SSPE buffer (20× SSPE contains 3.6 M NaCl, 0.2 M sodium phosphate, 0.02 M EDTA, pH 7.7) supplemented with 1% SDS, 100 μg/ml herring sperm DNA, and 5× Denhardt's reagent. Hybridization was performed for 16 h at 68 °C in the same solution plus the complete Zm*BT1*-cDNA fragment labeled by the random primer method with [α-^{32}P]dCTP using the Ready-To-Go prime kit (Amersham Biosciences). Afterward, the membranes were washed once at 37 °C for 15 min in 7× SSPE, 0.5% SDS and twice at 60 °C for 15 min in 0.1× SSPE, 1% SDS. Blots were visualized by a Cyclon PhosphorImager (Packard).

Quantitative Real-time RT-PCR—Total RNA was prepared from various maize tissues using the RNeasy Plant Mini Kit (Qiagen, Hilden, Germany). To remove any contaminating DNA, the samples were treated with deoxyribonuclease (RNase-free DNase Kit, Qiagen). Quantitative PCR was performed using MyIQ-Cycler (Bio-Rad) and IQ SYBR Green Supermix (Bio-Rad) according to the manufacturer's instructions with the following cycler conditions: 20 min at 50 °C; 15 min at 95 °C; 55 cycles: 15 s at 95 °C, 25 s at 58 °C, and 40 s at 72 °C. The sequences of the gene-specific oligonucleotides used for real-time RT-PCR are the following: Zm*BT1*-sense, 5′-CAAGGCTATCGAGCATTTCACC-3′; Zm*BT1*-antisense, 5′-TCGTAGGCGTAG-AAGTTACAGG-3′; Zm*BT1–2*-sense, 5′-AACAGCATATTACCCGTGGA-3′; Zm*BT1–2*-antisense, 5′-CCTCAGGCACGT-ACTTCATA-3′; *EF-1α*-sense, 5′-GCTTC-ACGTCCCAGGTCATC-3′ and *EF-1α*-antisense, 5′-TAGGCTTGGTGGGTATCA-TC-3′. The housekeeping gene in *Z. mays* encoding the elongation factor EF-1α (AF136829) was used for quantitative normalization. The specificity of the obtained RT-PCR products was controlled on 2% agarose gels.

Plasmid Construct for Heterologous Expression of ZmBT1 in E. coli—DNA manipulations were performed essentially as described by Sambrook *et al.* (20). The expression plasmid (pET 16b, Novagen, Heidelberg, Germany) encoding the recombinant ZmBT1 protein with an additional N-terminal tag of 10 histidine residues was constructed as follows: the cDNA coding the entire ZmBT1 was generated by PCR from first strand cDNA of maize endosperm tissue using *Pfu* DNA polymerase (Invitrogen). A sense primer including an NdeI restriction site and an antisense primer were used for the PCR (sense: 5′-GACTGAcatATGGCGGCGACAATG-3′; the lowercase letters indicate the introduced base exchange to create an NdeI restriction site; antisense: 5′-CTACCTTCTTGGCCAAGAACTTTG-3′). The obtained PCR product was purified (Nucleospin Extract II, Macherey & Nagel, Düren, Germany), subcloned into the EcoRV restriction site of the plasmid pBSK (Stratagene), and checked by sequencing on both strands by chain termination reaction (MWG-Biotech, Ebersberg, Germany). For the construction of the *E. coli* expression plasmid (encoding His_{10}-ZmBT1), the NdeI/BamHI DNA insert of the pBSK-plasmid was introduced in-frame into the corresponding restriction sites of the isopropyl β-D-thiogalactopyranoside (IPTG)-inducible T7-RNA polymerase bacterial expression vector pET16b (Novagen, Heidelberg, Germany). Transformations of *E. coli* were carried out according to standard protocols. The nucleotide sequence of the Zm*BT1* reported in this paper is available at the EMBL data base (www.ebi.ac.uk/embl/) under the accession number BT016796.

Heterologous Expression of ZmBT1 in E. coli—The *E. coli* strain Rosetta(DE3) was used for heterologous expression. The cDNA sequence encoding ZmBT1 under control of the T7-promoter was transcribed after IPTG induction of the T7-RNA polymerase (21). *E. coli* cells harboring the Zm*BT1* expression plasmid (or control expression plasmid pET16b) were grown at 37 °C in $TB^{Amp/Clm}$ medium (TB: 2.5 g/liter KH_2PO_4, 12.5 g/liter K_2HPO_4, 12 g/liter peptone, 24 g/liter yeast extract, 0.4% glycerin, pH 7.0). An optical density (A_{600}) of 0.5–0.6 was required for the initiation of T7-RNA polymerase expression by addition of IPTG (final concentration, 1 mM). Cells were grown for 1 h after induction and collected by centrifugation for 5 min at 4,000 × *g* (room temperature, Sorvall RC5B centrifuge, rotor type SS34; Sorvall-Du Pont, Dreieich, Germany). The pellet was resuspended to an A_{600} of 6 using potassium phosphate buffer (50 mM, pH 7.0) (22) and promptly used for uptake experiments.

Membrane integration of the recombinant full-length ZmBT1 in *E. coli* was confirmed by enrichment of the histidine-tagged protein and Western blot analysis using a ZmBT1 specific antibody (10). *E. coli* cells (20 ml) harboring the Zm*BT1* expression plasmid (or the pET16b control plasmid) were collected 1 h after IPTG induction (controls without IPTG) and transferred to liquid nitrogen to destroy cell intactness. After resuspension in a medium consisting of 10 mM Tris/HCl (pH 7.5), 1 mM EDTA, 0.1 mM Pefabloc, and 15% (v/v) glycerol, cells were further disrupted by ultrasonication (250 W, 3 × 30 s, 4 °C) and the suspension was centrifuged (10 min, 15,800 × *g*, 4 °C) to remove unbroken cells and inclusion bodies. Membranes extracted in the supernatant were sedimented for 45

min at 100,000 × *g* (TFT 80 rotor, Kontron Instruments, Munich, Germany), resuspended in binding buffer A consisting of 5 mM imidazole, 300 mM NaCl, 50 mM Na_2HPO_4 (pH 8.0, HCl), and 0.3% Triton X-100. After incubation on ice for 30 min, the not solubilized proteins were sedimented for 45 min at 100,000 × *g*. The solubilized histidine-tagged ZmBT1 in the supernatant was purified by nickel-chelating chromatography according to the supplier's instructions (Qiagen). Histidine-tagged protein was eluted with 500 μM imidazole and desalted by Sephadex G50 centrifugation. For SDS-PAGE, a protein aliquot was added to concentrated SDS-PAGE sample buffer medium and incubated for 30 min at room temperature. Finally, the preparation was applied to a polyacrylamide gel (3% stacking gel, 12% running gel) for electrophoresis in the presence of 0.1% SDS. Proteins were transferred to a nylon Hybond P membrane (Amersham Biosciences) in transfer buffer (39 mM glycine, 48 mM Tris base, 20% methanol, pH 8.3) for 1 h at 300 V. Western blot analysis was preformed utilizing a ZmBT1-specific antibody as primary antibody that was raised against 56 amino acids from the C terminus of the ZmBT1. An anti-rabbit IgG-alkaline phosphatase conjugate was used as secondary antibody. The immunoreactive bands were visualized by 5-bromo-4-chloro-3-indolyl phosphate and nitro blue tetrazolium substrate.

Transport Assays with E. coli—IPTG-induced *E. coli* cells (100 μl) harboring the Zm*BT1* expression plasmid (or the given controls) were added to 100 μl of potassium phosphate buffer (50 mM, pH 7.0) containing radioactively labeled ADP or ADP-Glc. [α-^{32}P]ADP was enzymatically synthesized from [α-^{32}P]ATP (PerkinElmer Life Sciences) as given in Tjaden *et al.* (17) and used at specific activities between 50 and 500 μCi/μmol. [^{14}C]ADP-Glc was used at specific activities between 20 and 250 μCi/μmol. Uptake of nucleotides was carried out at 30 °C in an Eppendorf reaction vessel incubator and terminated after the indicated time periods by transferring the cells to a 0.45-μm membrane filter (mixed cellulose ester, 25 mm diameter; Schleicher & Schuell, Dassel, Germany) under vacuum (23). Cells were further washed to remove unimported radioactivity by addition of 3 × 4-ml potassium phosphate buffer (50 mM, pH 7.0). The filter was subsequently transferred into a 20-ml scintillation vessel and filled with either 10 ml of water or 10 ml of scintillation mixture (Quicksafe A; Zinsser Analytic, Frankfurt/Main, Germany). Radioactivity in the samples was quantified in a Canberra-Packard Tricarb 2500 scintillation counter (Canberra-Packard, Frankfurt/Main, Germany). For efflux assays, *E. coli* cells were incubated with potassium phosphate buffer (50 mM, pH 7.0) containing 1 μM [^{14}C]ADP-Glc as a transport substrate. After the indicated time periods, the uptake medium was diluted with several unlabeled nucleotides to a final concentration of 1 mM and the efflux of [^{14}C]ADP-Glc was monitored at the given time points. Efflux was measured by membrane filtration as described above. To analyze the degree of metabolic conversion of imported [^{14}C]ADP-Glc, we carried out a thin layer chromatography according to the method of Mangold (24).

Sequence Analysis—Multiple alignments of amino acid sequences from known BT1 homologues available at the EMBL data base (www.ebi.ac.uk/embl/) were obtained using Clustal X (25). The phylogenetic tree was created with PhyML (26) after aligning the sequences with Muscle (27).

RESULTS

Sequence Analysis of ZmBT1—The Zm*BT1* cDNA clone was isolated from the first strand cDNA of maize endosperm as given under "Experimental Procedures." Six independent PCR products of Zm*BT1* have been sequenced and found to exhibit 100% identity excluding failure of the *Pfu* polymerase. Compared with the open reading frame of the Zm*BT1* sequence published by Sullivan *et al.* (28), our Zm*BT1* cDNA sequence differs in the following positions: six additional nucleotides (G at bp position 246, 295, and 411, and GGA at bp position 1257–1259) and two nucleotide changes (GC instead of CG at bp position 338–339). The resultant triple frameshift modified the deduced amino acid sequence ahead of the first predicted transmembrane domain (amino acid position 83–137) and the additional amino acid residue at the C terminus (position 419) led to a substantial higher similarity to other BT1 isoforms (Fig. 1). Interestingly, the Zm*BT1* cDNA sequence we determined was recently submitted by Lai *et al.* as well (2004, direct submission, accession number BT016796, www.ncbi.nlm.nih.gov). The deduced ZmBT1 protein sequence was aligned with putative BT1 homologues from wheat (*Triticum aestivum*), rice (*Oryza sativa*), barley (*Hordeum vulgare*), maize (*Z. mays*), barrel medic (*Medicago truncatula*), potato (*S. tuberosum*), and *Arabidopsis thaliana* (Fig. 1).

The amino acid sequence of the BT1 homologues consists of three tandem repeats of ~100 residues showing 6 putative transmembrane helices (15). All BT1 homologues possess three conserved mitochondrial energy transfer signatures that are characteristic for membrane proteins belonging to the mitochondrial carrier family (29, 30). Phylogenetic analyses classify BT1 homologues as members of the mitochondrial carrier family forming a monophyletic cluster (31). A comparison of the BT1 isoforms revealed a high similarity of ZmBT1 to TaBT1 (66% identity, 75% similarity), OsBT1-1 (66% identity, 73% similarity), HvNST (65% identity, 74% similarity), and to a lower extent to OsBT1–3 (58% identity, 68% similarity), ZmBT1–2 (58% identity, 68% similarity), OsBT1–2 (48% identity, 60% similarity), MtBT1 (46% identity, 63% similarity), StBT1 (45% identity, 61% similarity), and AtBT1 (44% identity, 61% similarity). Phylogenetic analyses of the BT1 homologues indicate that the BT1 protein family can be divided into two subgroups. The first phylogenetic cluster comprises only BT1 homologues from monocotyledonous plants including ZmBT1 (Fig. 2). The second cluster includes BT1 homologues from both mono- and dicotyledonous plants indicating a putative distinct function compared with the monocotyledonous-specific group (Fig. 2).

Several computer programs (*i.e.* ChloroP 1.1, PredSL, etc.) predict for all BT1 homologues a plastidic localization due to the N-terminal plastidic transit peptides (32, 33). For ZmBT1, HvNST1, and StBT1, a plastidic localization was experimentally verified by immunological studies, green fluorescent protein fusion, and/or targeting experiments into isolated plastids (9, 15, 34).

Southern Blot Analysis of ZmBT1 in Maize—In the light of the differences registered between *BT1* gene copy numbers in

mono- and dicotyledonous plants based on the rice and *Arabidopsis* genomes (35, 36), we assessed *BT1* gene copy numbers in maize by Southern blot analyses. We chose restriction enzymes that do cut either Zm*BT1* or the recently published Zm*BT1–2* homologue (accession number BT016800). The digestion of the genomic maize DNA with the restriction enzymes (XbaI, XhoI, and HindIII) led to two distinct bands on the Southern blot (Fig. 3, *lanes 1–3*). Only digestion with BamHI showed three bands, which is most probably due to a restriction site inside an intron of one of the two *BT1* homologues. These results clearly indicate that two BT1 homologues occur in maize, in contrast to one homologue in dicotyledonous plants (15) (Fig. 2) and three homologues in rice (35).

Heterologous Expression of ZmBT1 in E. coli Cells—We showed previously that the heterologous synthesis of the plastidic StBT1 homologue in *E. coli* leads to the functional integration of StBT1 into the bacterial cytoplasmic membrane (15). Astonishingly, we identified StBT1 as a plastidic adenine nucleotide uniporter despite the attributed function to BT1 proteins to transport ADP-Glc in counterexchange with ADP and/or AMP (14, 34, 37). However, a high degree of sequence similarity for homologues belonging to the same protein family cannot be taken as proof for the same function (see Ref. 38), specifically when there are multiple homologues per genome indicating paralogy and potential functional differentiation between the homologues. The kinetic properties as well as the substrate specificity should be identified for each putative homologue.

The heterologous expression of Zm*BT1* in different *E. coli* strains was analyzed using a peptide-specific antibody raised against a fusion protein including the 56 amino acid residues in the C-terminal sequence of ZmBT1. Substantial differences in the expression level of carrier

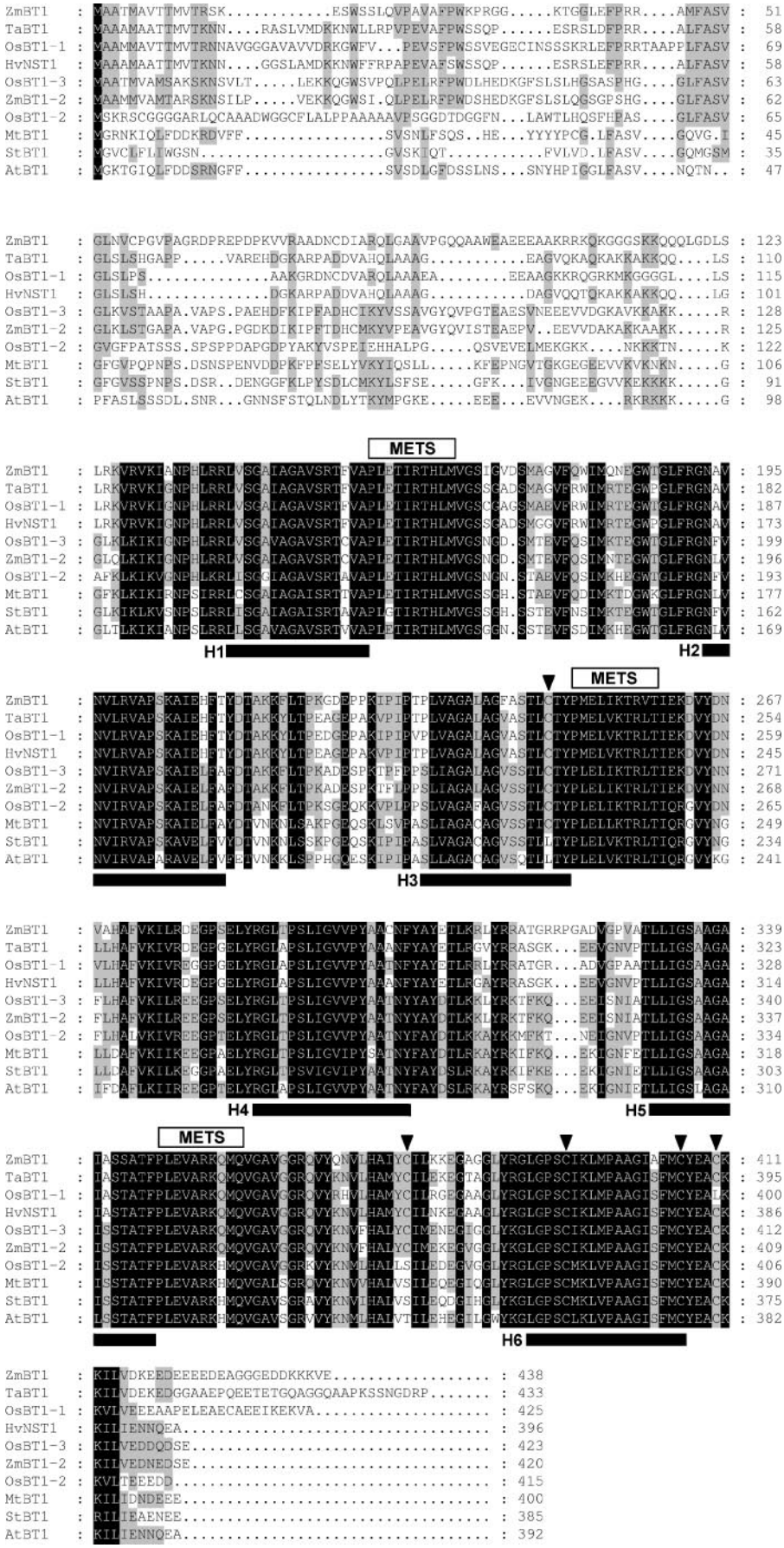

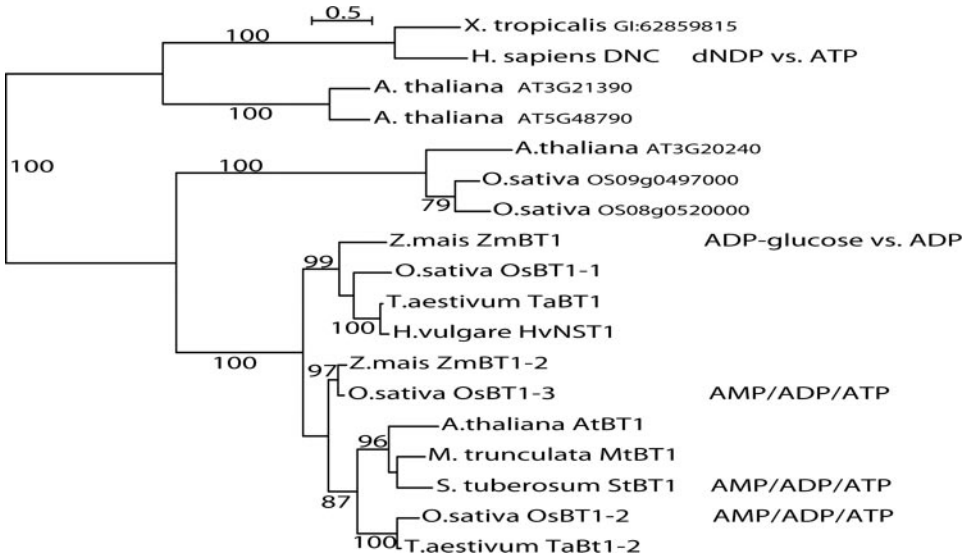

FIGURE 2. **Phylogeny of the Brittle1 proteins.** A phylogeny was created with PhyML (26) after aligning the sequences with Muscle (27). The PhyML phylogeny was created with 2 γ-distributed rate parameters and the JTT model for amino acid substitutions. Bootstrap values above 85 out of 100 are indicated. A phylogeny created with Neighbor Joining using the identity matrix and correcting for multiple replacements had an identical topology. The phylogeny indicates a split between the AMP/ADP/ATP carriers and the ADP-glucose carriers, although the exact division between the groups as indicated in the tree is not very strongly supported. The extra sequences are a plant specific group (*Arabidopsis* and rice) of unknown function that is phylogenetically close to the Brittle1 group. The deoxynucleotide carrier group was used as outgroup because it is phylogenetically closest in a phylogeny of the 500 "best hits" to the Brittle1 group of proteins. At the *right*, experimentally determined substrate specificity of the carriers are indicated. Accession numbers of the BT1 proteins are given in the legend to Fig. 1 with the exception of TaBT1–2 (NCBI accession number BT009587), which is not a full-length clone.

proteins in *E. coli* have been reported (18, 39), probably due to the unfavorable codon usage of several carrier proteins in *E. coli* (39). In fact, a screening of the Zm*BT1* cDNA sequence revealed several codons rarely used in *E. coli* so that synthesized ZmBT1 protein in BL21, the most widely used expression host, was hard to detect (data not shown). In marked contrast, the use of *E. coli* Rosetta strains, which carry the pRARE plasmid and thus supply tRNAs for codons rarely used in *E. coli*, allows a high expression of Zm*BT1*. We confirmed the integration of the heterologously expressed ZmBT1 in the *E. coli* Rosetta cytoplasmic membrane by Western blotting by use of the above mentioned peptide-specific ZmBT1 antibody (Fig. 4).

We tested ADP-Glc as a putative transport substrate for ZmBT1. Uptake of [^{14}C]ADP-Glc into *E. coli* Rosetta cells harboring ZmBT1 in their membranes was linear with time for at least 15 min. The ADP-Glc uptake was strictly dependent on the membrane intactness and ZmBT1 protein synthesis (supplementary materials Fig. 1). Thus, we analyzed the affinity for ADP-Glc at different substrate concentrations. The results are given in Fig. 5*A*. Increased exogenous radioactively labeled ADP-Glc induced increased rates of ADP-Glc transport into *E. coli* cells harboring ZmBT1. Lineweaver-Burk analyses revealed an apparent K_m value for ADP-Glc of 847.8 $\pm$ 39.6 μM and a V_{max} of 191.5 $\pm$ 28.7 nmol of ADP-Glc/mg of protein^{-1} h^{-1} (Fig. 5*A*).

To investigate the substrate specificity of ZmBT1, we measured the effect of various non-labeled metabolic intermediates on the rate of [^{14}C]ADP-Glc uptake (Table 1). Substantial inhibition of [^{14}C]ADP-Glc import could be observed with non-labeled ADP and ADP-Glc reducing the transport rate below 15 and 24% of the control (without effector), respectively. None of the other metabolic intermediates tested showed any substantial influence on [^{14}C]ADP-Glc uptake, which confirms ADP-Glc and ADP as the main substrates for ZmBT1 (Table 1). Furthermore, we analyzed the affinity of ZmBT1 for ADP (Fig. 5*B*). Increased exogenous radioactively labeled ADP induced increased rates of ADP transport into *E. coli* cells harboring ZmBT1. Lineweaver-Burk analyses revealed an apparent K_m value for ADP of 465.2 $\pm$ 36.2 μM and a V_{max} of 6.1 $\pm$ 0.7 nmol of ADP/mg of protein^{-1} h^{-1} (Fig. 5*B*). The higher affinity for ADP compared with ADP-Glc is reflected in the competition experiments of ADP-Glc uptake (Table 1). The substantial higher maximal velocity of ADP-Glc uptake seems to be a particular feature of this carrier (Fig. 5). Thus, the resulting relative catalytic efficiency (V_{max}/K_m) of ZmBT1 is 18 times higher for ADP-Glc than for ADP.

Biochemical studies on isolated maize endosperm plastids led to the assumption that ADP-Glc is transported across the envelope membranes in counterexchange with ADP or AMP (37). AMP can be excluded as exogenous substrate for ZmBT1 because we could not detect any substantial inhibition of non-labeled AMP on the ADP-Glc uptake or any direct uptake of radioactively labeled [^{14}C]AMP into *E. coli* cells harboring ZmBT1 (Table 1, data not shown). However, we could also exploit the *E. coli* system to investigate the counterexchange properties of the heterologously synthesized ZmBT1. The principle of this approach is to initiate a putative efflux of imported radioactively labeled [^{14}C]ADP-Glc through a high dilution

FIGURE 1. **Alignment of the predicted amino acid sequence of ZmBT1 with BT1 homologues.** The residues identical or similar among all family members are indicated by *black shading* and the residues conserved by at least five proteins are shaded in *gray shading*. *Solid black bars* underline six putative membrane-spanning regions (H1–H6). Three conserved mitochondrial energy transfer signatures (METS = P*X*(DE)*X*(LIVAT)(RK)*X*(LRH)(LIVMFY)(QGAIVM)), following each odd membrane-spanning domain are marked by *white bars*. Conserved cysteine residues are indicated by *triangles*. *Dashes* represent gaps introduced to improve the similarity among the proteins. The *numbers* indicate the amino acid positions. *ZmBT1*, Brittle1 from *Zea mays* (NCBI accession number BT016796); *TaBT1*, Brittle1 from *T. aestivum* (NCBI accession number BT008958); *OsBT1–1*, Brittle1–1 from *Oryza sativa* (NCBI accession number BAD15863); *HvNST1*, nucleotide sugar transporter (brittle1) from *H. vulgare* (NCBI accession number AAT12275); *OsBT1–3*, Brittle1 from *O. sativa* (NCBI accession number BAD15863); *ZmBT1–2*, Brittle1–2 from *Z. mays* (NCBI accession number BT016800); *OsBT1–2*, Brittle1–2 from *O. sativa* (NCBI accession number AAU44334); *MtBT1*, Brittle1 from *M. truncatula* (NCBI accession number ABE88494); *StBT1*, Brittle1 from *S. tuberosum* (NCBI accession number CAA67107); *AtBT1*, Brittle1 from *A. thaliana* (NCBI accession number CAB79957).

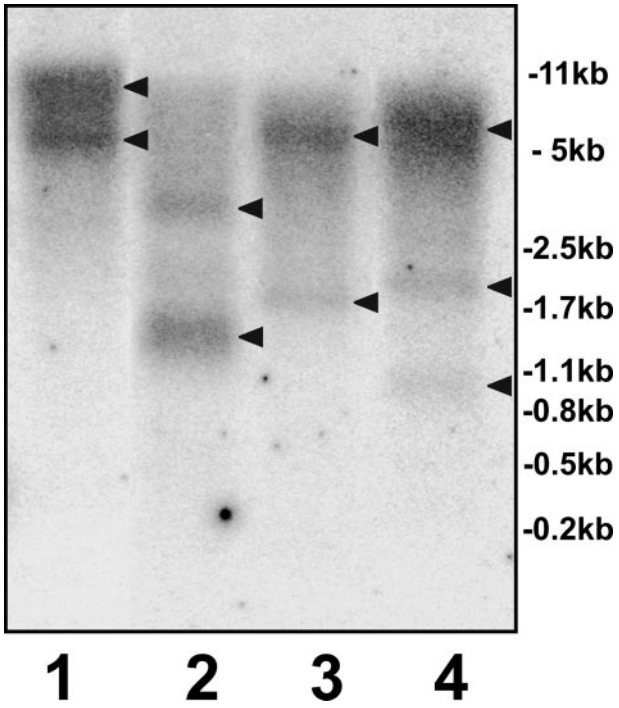

FIGURE 3. **Genomic Southern analysis of maize DNA.** Nuclear DNA of *Z. mays* was digested with XbaI (*lane 1*), XhoI (*lane 2*), HindIII (*lane 3*), and BamHI (*lane 4*), and subjected to Southern analysis. The coding region of Zm*BT1* cDNA was radioactively labeled and used as hybridization probe. The sizes of DNA molecular mass standards are indicated.

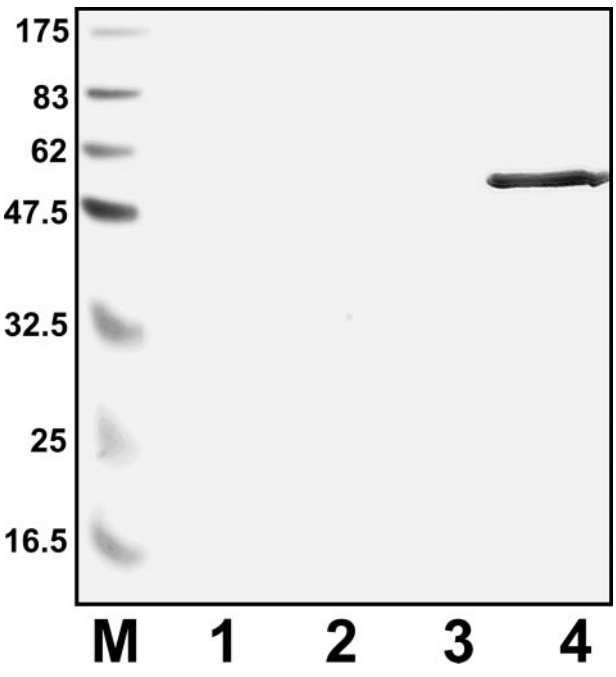

FIGURE 4. **Western blot analysis of ZmBT1 heterologously expressed in *E. coli* Rosetta cells.** *E. coli* cells harboring the plasmid encoding ZmBT1 and *E. coli* control cells (pET16b without any insert) were induced by application of IPTG for protein synthesis. Details of induction, purification, and Western blotting are given under "Experimental Procedures." Immunoblotting was carried out with a ZmBT1-specific antiserum. *Lane 1*, membrane fraction of uninduced *E. coli* control cells; *lane 2*, membrane fraction of IPTG-induced *E. coli* control cells; *lane 3*, membrane fraction of uninduced *E. coli* cells harboring the plasmid encoding ZmBT1; *lane 4*, membrane fraction of IPTG-induced *E. coli* cells harboring the plasmid encoding ZmBT1.

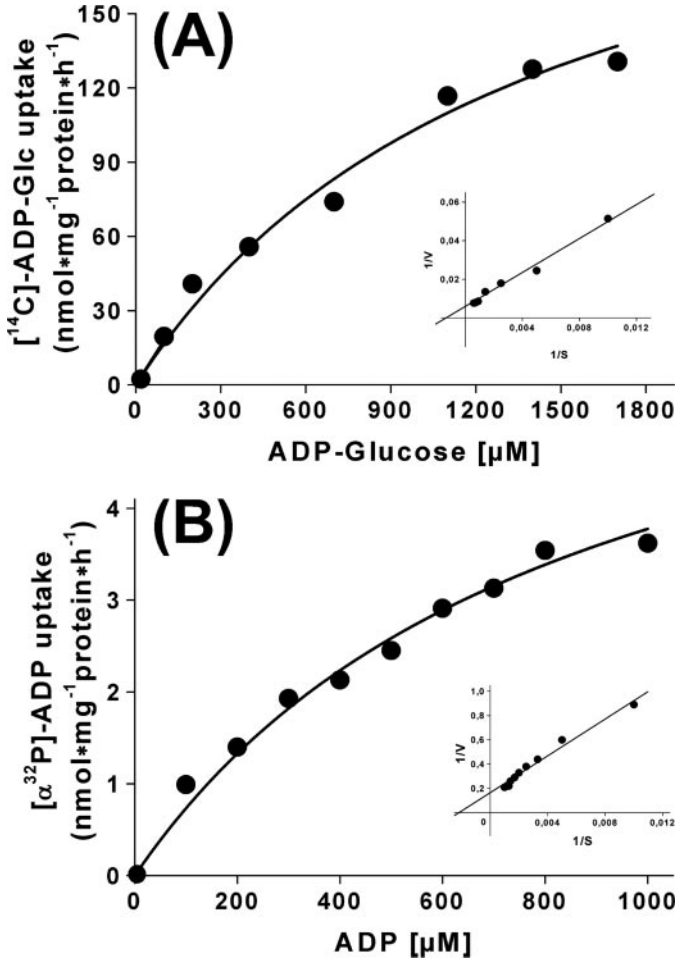

FIGURE 5. **Substrate saturation of ADP-Glc and ADP uptake into intact *E. coli* cells.** IPTG-induced *E. coli* cells harboring the plasmid encoding ZmBT1 were incubated for 8 min with the indicated concentrations of [^{14}C]ADP-Glc (*A*) or [α-^{32}P]ADP (*B*). Data are the mean of three independent experiments with four replicates each. Background rates of the control (pET16b without insert) have been subtracted. The *insets* represent a double reciprocal plot of the data for uptake indicating a K_m value for ADP-Glc of 847.8 $\pm$ 39.6 μM with a V_{max} of 191.5 $\pm$ 28.7 nmol of ADP-Glc/mg of protein^{-1} h^{-1} (*A*) and a K_m value for ADP of 465.2 $\pm$ 36.2 μM with a V_{max} of 6.1 $\pm$ 0.7 nmol of ADP/mg of protein^{-1} h^{-1} (*B*).

(chase) with non-labeled substrates at a certain time point during an uptake experiment (15, 22). To analyze whether imported [^{14}C]ADP-Glc is metabolized by *E. coli* cells harboring ZmBT1, we disrupted the cells at several time points after preloading with [^{14}C]ADP-Glc and analyzed the cytosolic fraction by thin layer chromatography. Most of the [^{14}C]ADP-Glc (about 90%) was found not to be metabolized by the *E. coli* cells over a time span of about 12 min, which suggests the involvement of [^{14}C]ADP-Glc in a putative nucleotide exchange (Fig. 6*A*). Fig. 6*B* shows a typical time course for [^{14}C]ADP-Glc uptake (at 1 μM) into *E. coli* cells harboring ZmBT1. Right after the start of the chase with non-labeled ADP (1 mM), a rapid efflux led to a total release of labeled nucleotides of about 65% (7 min after the start of the chase). GTP, used as a control, is known not to be a substrate for ZmBT1 (Table 1) and, therefore, showed no influence on the uptake of radioactively labeled ADP-Glc after the chase. These results clearly reveal that ZmBT1 mediates a counterexchange of ADP-Glc and ADP. Non-labeled ADP-Glc (1 mM) inhibited significantly the

TABLE 1

Effects of various metabolites on [^{14}C]ADP-glucose transport activities of ZmBT1

Metabolic effectors were given at a concentration of 1 mM. [^{14}C]ADP-glucose was present at a concentration of 200 μM. Uptake into IPTG-induced *E. coli* cells harboring ZmBT1 was carried out for 8 min and stopped by rapid filtration (see "Experimental Procedures"). Data are the mean of three independent experiments with four replicates each. S.E. is less than 8% of the mean values.

Effector	Rate of transport
	%
None	100.0
ADP	14.5
ADP-Glc[a]	23.9
ATP	70.8
AMP[b]	82.3
UDP-Glc	98.2
UDP-Gal	92.6
Adenosine	91.1
Adenine	90.1
GTP	101.1
CTP	101.6
UTP	99.7
IDP	95.3
NADP	98.9
NADPH	89.9

[a] ADP-Glc value is corrected by inhibition (0.5%) of the contamination with ATP, ADP, and AMP.

[b] AMP value was determined at the presence of 1 mM adenosine (to prevent the cleavage of AMP by *E. coli* cells (15)) and corrected by the adenosine inhibition of 8.9%.

[^{14}C]ADP-Glc uptake mediated by ZmBT1 but did not initiate any exchange of ADP-Glc (Fig. 6*B*).

Due to the fact that commercially available ADP-Glc is contaminated by other adenylates, namely AMP, ADP, and ATP (15), we determined the contamination of ADP-Glc by high performance liquid chromatography analysis (1.8% ADP; 0.6% ATP; 0.5% AMP) and carried out the same experiment using the calculated nucleotide contaminations as a non-labeled nucleotide mixture (18 μM ADP, 6 μM ATP, and 5 μM AMP) for the chase during [^{14}C]ADP-Glc uptake. The chase with this nucleotide mixture did not lead to any competitive inhibition of [^{14}C]ADP-Glc uptake, so that the above mentioned competitive inhibition of non-labeled ADP-Glc is not influenced by the contamination (Fig. 6*B*). These results indicate a selective exchange of ADP-Glc with ADP. To further validate this mode of transport we preloaded *E. coli* cells harboring ZmBT1 with 500 μM non-labeled exogenous ADP for 5 and 10 min, washed the cells, and performed [^{14}C]ADP-Glc uptake in comparison to not preloaded cells. Indeed, [^{14}C]ADP-Glc uptake into *E. coli* cells harboring ZmBT1 increased up to 174% compared with the control when the cells were preloaded with the counterexchange substrate ADP (Fig. 6*C*). To clarify whether endogenous AMP might have an influence on [^{14}C]ADP-Glc uptake into *E. coli* cells harboring ZmBT1 we preloaded these cells with 1 mM non-labeled exogenous AMP for 5 and 10 min, washed the cells, and performed [^{14}C]ADP-Glc uptake in comparison to non-preloaded cells (supplementary materials Fig. S2). In strong contrast to the experiment with ADP-preloaded cells (Fig. 6*C*), additional endogenous AMP has no influence on the ZmBT1 mediated ADP-Glc uptake (supplementary materials Fig. S2*B*).

We also determined the influence of several inhibitors on [^{14}C]ADP-Glc uptake (Table 2). The highly specific inhibitors of the mitochondrial ADP/ATP carriers (AACs), bongkrekic acid and carboxyatractyloside (40, 41), showed

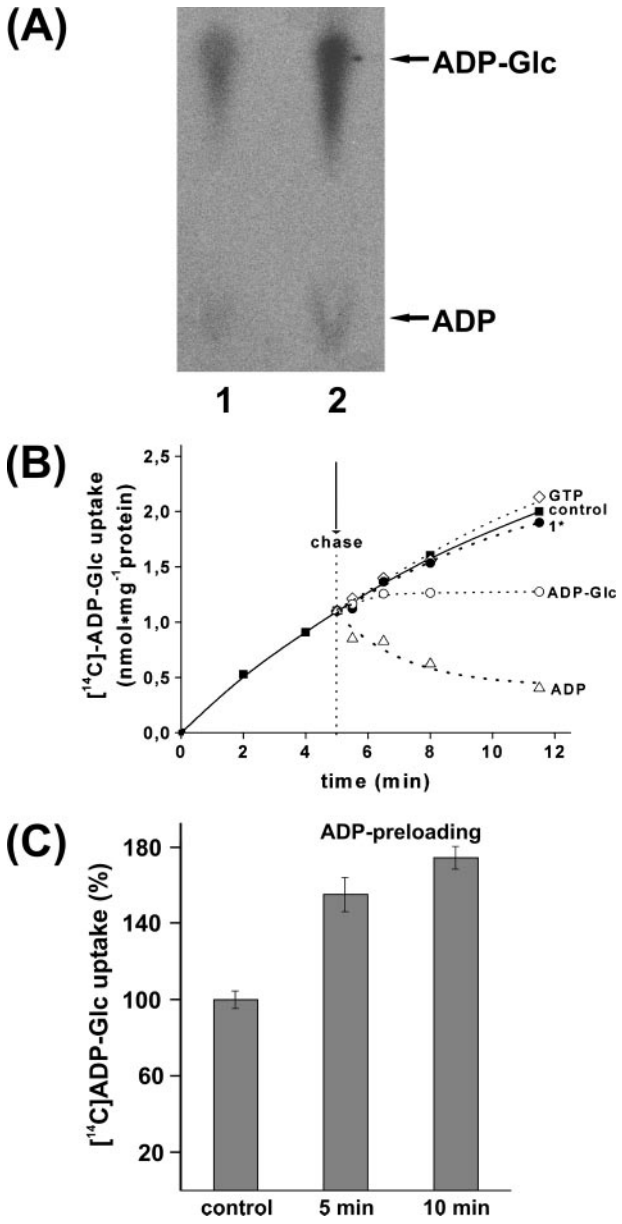

FIGURE 6. **Exchange-mediated efflux studies of intracellular radioactivity.** *A*, *E. coli* cells harboring ZmBT1 were disrupted after preloading with 1 μM [^{14}C]ADP-Glc for 3 (*lane 1*) and 12 min (*lane 2*), and the cytosolic radioactively labeled compounds were separated by thin-layer chromatography. Most of the imported ADP-Glc (90%) was found not to be metabolized. Cells used were harvested in the exponential phase that leads to a negligible glycogen synthase activity. *B*, *E. coli* cells harboring ZmBT1 were incubated in the presence of 1 μM [^{14}C]ADP-Glc. After 5 min of [^{14}C]ADP-Glc incubation, unlabeled nucleotides were added (chase) to a final concentration of 1 mM (1000-fold) and a possible induced efflux was monitored for the given time span. Data are the mean of three independent experiments with four replicates each. S.E. values were less than 8% of the mean values. *1**, the contamination of 1 mM ADP-Glc was determined by high performance liquid chromatography analysis; the corresponding concentrations of 18 μM ADP, 6 μM ATP, and 5 μM AMP were added and monitored as described above for all unlabeled nucleotides. *C*, *E. coli* cells harboring ZmBT1 were preloaded with 500 μM non-labeled exogenous ADP for 5 and 10 min. After washing the preloaded cells, [^{14}C]ADP-Glc uptake was measured as above for 8 min in comparison to not ADP preloaded cells (control). Data are the mean ± S.E. of three independent experiments with four replicates each. *Lane 1*, [^{14}C]ADP-Glc uptake into *E. coli* control cells harboring ZmBT1 (100% uptake = 1.56 nmol of ADP-Glc/mg of protein^{-1}); *lane 2*: [^{14}C]ADP-Glc uptake into *E. coli* cells harboring ZmBT1 (5 min preloaded); *lane 3*, [^{14}C]ADP-Glc uptake into *E. coli* cells harboring ZmBT1 (10 min preloaded).

TABLE 2

Effects of various inhibitors on [^{14}C]ADP-glucose transport activities of ZmBT1

[^{14}C]ADP-glucose uptake into IPTG-induced *E. coli* cells harboring ZmBT1 was measured at a concentration of 200 μM. *E. coli* cells were preincubated for 10 min with lysozyme (1.25 mg/ml) to allow penetration of the reagents across the outer membrane. Uptake was carried out for 8 min and stopped by rapid filtration (see "Experimental Procedures"). The inhibitors were used in following concentrations: bongkrekic acid (BKA, 10 μM); carboxyatractyloside (CAT, 1 mM); pyridoxal 5′-phosphate (PLP, 2 mM), and mersalyl (100 μM). Data are the mean of three independent experiments with four replicates each. S.E. is less than 9% of the mean values.

Effector	Rate of transport
	%
None	100.0
BKA	109.5
CAT	88.1
PLP	91.4
Mersalyl	11.6

no inhibitory effect at the given concentrations (Table 2). In addition, no considerable inhibition was observed with pyridoxal 5′-phosphate, a potential inhibitor of StBT1 and the plastidic phosphate translocators (15, 42) (Table 2). Interestingly, the sulfhydryl reagent mersalyl, which is known to initiate a blockage of thiol groups (43), significantly inhibited the [^{14}C]ADP-Glc transport mediated by ZmBT1 below 12% of the control (Table 2). This indicates that SH-groups are of considerable importance for the activity of the ZmBT1.

The activity of various chloroplast enzymes is known to be regulated by reversible thiol-disulfide interchange mediated by the ferredoxin-thioredoxin system (44). Recent studies on wheat starchy endosperm amyloplasts suggest also a thioredoxin (Trx) regulation of proteins in heterotrophic tissues. 42 amyloplast proteins were identified as potential Trx target proteins using a proteomic approach in combination with affinity chromatography and a fluorescent thiol probe (1). Interestingly, BT1, a major envelope protein of wheat amyloplasts, was also recognized as a thioredoxin target protein (1). To determine whether the activity of ZmBT1 is dependent on the redox state, we performed uptake of [^{14}C]ADP-Glc into *E. coli* Rosetta cells harboring ZmBT1 in the presence of diamide and/or dithiothreitol (DTT). In *E. coli*, the thioredoxin and glutaredoxin systems are known to keep reduced conditions for cytoplasmic proteins (45). This implicates that in ZmBT1 a disulfide bond formation is prevented under normal *E. coli* growth conditions. The addition of the membrane-permeant thiol-specific oxidizing agent diamide (diazenedicarboxylic acid bis(*N*,*N*′-dimethylamide) (45)) during the uptake experiments causes a strong inhibition of ADP-Glc uptake of *E. coli* Rosetta cells harboring ZmBT1 (Fig. 7*A*). At a concentration of 10 mM diamide the ADP-Glc uptake mediated by ZmBT1 is decreased up to 50%. In control experiments we confirmed the specificity of this effect on ZmBT1. The mitochondrial ADP/ATP carrier AAC2 from *A. thaliana* is not influenced by 10 mM diamide when heterologously synthesized in *E. coli* (Fig. 7*A*). Interestingly, the inhibition of ADP-Glc uptake into *E. coli* Rosetta cells harboring ZmBT1 was shown to be reversible. The decrease of ADP-Glc uptake mediated by ZmBT1 after preincubation with 10 mM diamide was mainly compensated by the addition of 40 mM reduced DTT (Fig. 7*B*). The addition of 40 mM DTT (without diamide preincubation) does not affect any ADP-Glc uptake into *E. coli* Rosetta cells harboring ZmBT1, which indicates an optimal activation of ZmBT1 by reduced conditions in these *E. coli* expression cells (Fig. 7*B*).

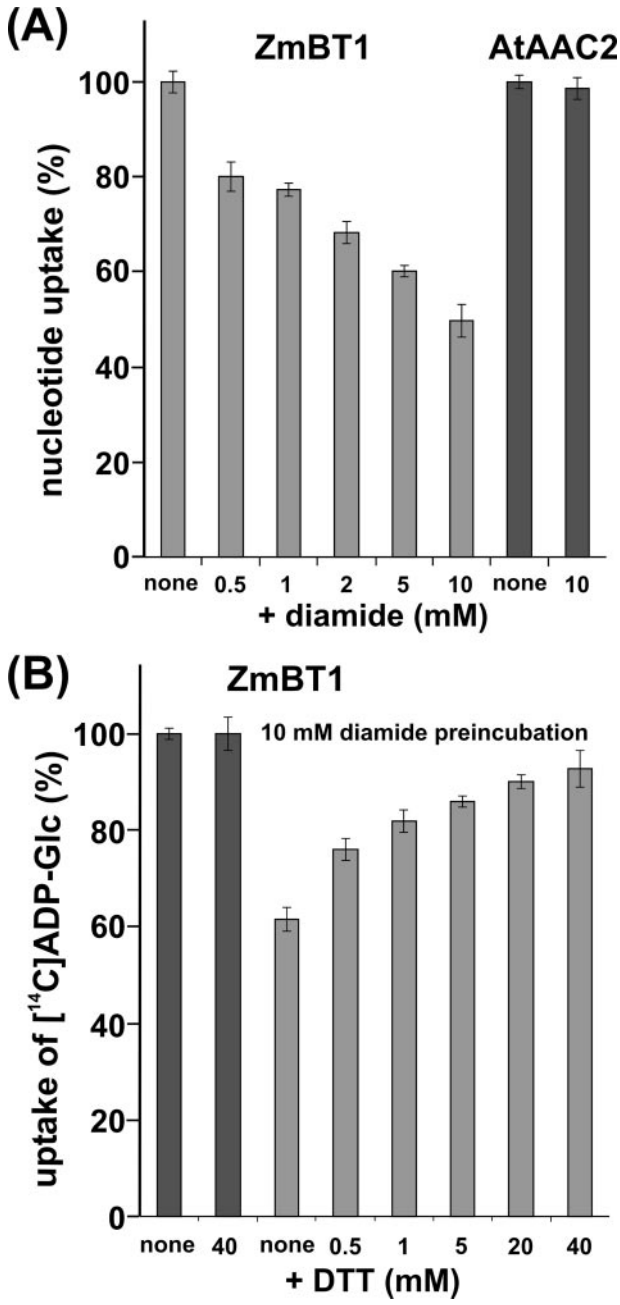

FIGURE 7. **Effects of diamide and DTT on [^{14}C]ADP-Glc uptake into intact *E. coli* cells harboring ZmBT1.** *A*, IPTG-induced *E. coli* cells harboring ZmBT1 (*gray bars*) were incubated with 200 μM [^{14}C]ADP-Glc for 8 min in the presence of indicated diamide concentrations. As control, IPTG-induced *E. coli* cells harboring AtAAC2 (*black bars*) were incubated with 15 μM [α-^{32}P]ADP for 8 min in the presence of the indicated diamide concentrations. Data are the mean ± S.E. of three independent experiments with four replicates each. *B*, IPTG-induced *E. coli* cells harboring ZmBT1 (*gray bars*) were preincubated with 10 mM diamide (for 3 min) before incubation with 200 μM [^{14}C]ADP-Glc for 8 min in the presence of the indicated DTT concentrations. As control, IPTG-induced *E. coli* cells harboring ZmBT1 (*black bars*) were incubated with 200 μM [^{14}C]ADP-Glc for 8 min in the presence of the indicated DTT concentrations without diamide preincubation. Data are the mean ± S.E. of three independent experiments with four replicates each.

Expression Analyses of ZmBT1 and the BT1 Maize Homologue, ZmBT1–2, in Different Maize Tissues—To obtain further insight into the putative physiological roles of ZmBT1 and the recently identified ZmBT1–2 homologue, we analyzed the accumulation of the corresponding mRNAs in various autotrophic and heterotrophic tissues. Gene expression levels of low abundant proteins can be determined by real-time RT-PCR, which is more specific and sensitive than Northern blot analyses (15, 46). The use of the total RNA mass (or 18 S rRNA) for normalization might be misleading because it consists predominantly of rRNA molecules that are often not representative for the mRNA fraction in different plant tissues (47). A reliable internal control should be similarly expressed in different cell types (48). Therefore, we chose the elongation factor EF-1α, which catalyzes the first step of protein synthesis by binding the aminoacyl-tRNA to the aminoacyl site of ribosomes. EF-1α is described to be a suitable housekeeping gene commonly used in plants as an internal control for real-time RT-PCR (48–50).

The real-time RT-PCR quantification shows an exclusive expression of Zm*BT1* in maize endosperm tissues (15 days after pollination), which indicates an essential role for ZmBT1 in starch metabolism as reported earlier (10, 14). In strong contrast, the Zm*BT1–2* homologue is expressed in heterotrophic and autotrophic tissues indicating a general role in plant metabolism that was also observed for the BT1 homologues of potato (StBT1), *Arabidopsis* (AtBT1), and rice (OsBT1–2 and OsBT1–3) (15, 35).

DISCUSSION

The ADP-Glc required for starch synthesis in plastids of cereal endosperm is mainly synthesized in the cytosol and has to be transported across the plastid envelope (2, 51, 52). Physiological studies on maize and barley mutants postulate that BT1 homologues are involved in the ADP-Glc transport (14, 34, 37). However, a conclusive proof that BT1 is the ADP-Glc transporter and a detailed analysis of this protein on the molecular level are still lacking.

In this paper, we have investigated the biochemical characteristics of the maize BT1 homologue ZmBT1 (Fig. 1). Heterologous synthesis of ZmBT1 in *E. coli* leads to the functional integration into the bacterial cytoplasmic membrane (Figs. 4 and 5). Uptake experiments on intact *E. coli* cells harboring ZmBT1 clearly reveal a high substrate specificity of ZmBT1 for ADP-Glc and ADP with affinities of about 850 and 465 μM, respectively (Fig. 5; Table 1). After preloading *E. coli* cells harboring ZmBT1 with radioactively labeled [^{14}C]ADP-Glc, efflux was initiated by addition of non-labeled ADP (Fig. 6*B*). Interestingly, a chase with 1000-fold non-labeled ADP-Glc did not cause any efflux of radioactively labeled [^{14}C]ADP-Glc but completely inhibited any further [^{14}C]ADP-Glc uptake. Furthermore, uptake of [^{14}C]ADP-Glc into *E. coli* cells harboring ZmBT1 was stimulated when cells were preloaded with non-labeled ADP as a putative counterexchange substrate (Fig. 6*C*). These results characterize ZmBT1 as a carrier that mediates a strict counterexchange of ADP-Glc with ADP. Thus, ZmBT1 is here identified as an ADP-Glc transporter that enables ADP-Glc import into cereal endosperm plastids in exchange with ADP, which is generated during the ADP-Glc-dependent starch synthesis inside plastids (14, 37).

Recently, efflux experiments on isolated wheat amyloplasts revealed that during the ADP-Glc-dependent starch synthesis ADP is the major adenylate exported from intact amyloplasts (53). The comparable low affinity of ZmBT1 for ADP-Glc (850 μM) seems to be sufficient for effective transport due a highly active cytosolic ADP-Glc pyrophosphorylase (AGPase), which maintains high concentrations of ADP-Glc in the cytosol of maize endosperm (51–54).

The components of a complete ferredoxin/thioredoxin system have been recently identified in amyloplasts isolated from wheat starchy endosperm. In cereal endosperm, ferredoxin is reduced not by light, as in chloroplasts, but by the metabolically generated NADPH via ferredoxin NADP reductase (1). Interestingly, the wheat BT1 was revealed as a potential Trx target protein (1). BT1 homologues possess several conserved cysteins, which is a prerequisite for the presence of a regulatory disulfide bond (Fig. 1). The inhibition and the reversible activation of ZmBT1 by diamide and DTT provide the first experimental evidence that the ADP-Glc carrier from cereal endosperm is in fact redox regulated as postulated for the wheat BT1 (Fig. 7). However, the specific cysteine residues that are involved in the redox regulation of ZmBT1 have still to be identified. Therefore, we aim at generating ZmBT1 Cys mutants by site-directed mutagenesis for further functional analyses.

The reducing power (NADPH) for the activation of the ADP-Glc carrier from cereal endosperm is derived from the oxidative pentose phosphate pathway residing in amyloplasts (55). NADPH is generated enzymatically by glucose 6-phosphate and 6-phosphogluconate dehydrogenases after import of Glc-6-P (56, 57). In this context, the high expression of the glucose 6-phosphate/phosphate transporter in developing maize kernels makes sense. Glc-6-P imported by this carrier is used for the oxidative pentose phosphate pathway and not for the starch synthesis (57, 58).

The regulation of BT1 gained prominence in subsequent studies showing that the cytosol, rather than the plastid, is the major site of ADP-Glc formation in cereal endosperm (2). Thus, the regulation of the BT1-mediated ADP-Glc transport into cereal endosperm plastids is of high physiological importance. The transport of sucrose into sink tissues such as endosperm would finally increase the NADPH/NADP ratio, which indicates a high energy status of the plant cells leading to a higher starch synthesis via the Trx-regulated ADP-Glc transport into heterotrophic plastids (1).

The occurrence of BT1 homologues in non-cereal plants such as *A. thaliana*, *S. tuberosum*, and *M. truncatula* was first unexplainable because in these plants ADP-Glc was not imported into the storage plastids for starch synthesis due to the plastidic localization of the AGPase. Recently, a BT1 homologue from a dicotyledonous plant, the StBT1 from potato, was characterized as a novel plastidic adenine nucleotide uniporter used to provide the cytosol and other compartments with adenine nucleotides exclusively synthesized inside plastids (15). Because the *de novo* purine nucleotide metabolism is of general importance in all plants, one should expect this novel type of plastidic carriers also in cereals. This implicates that maize

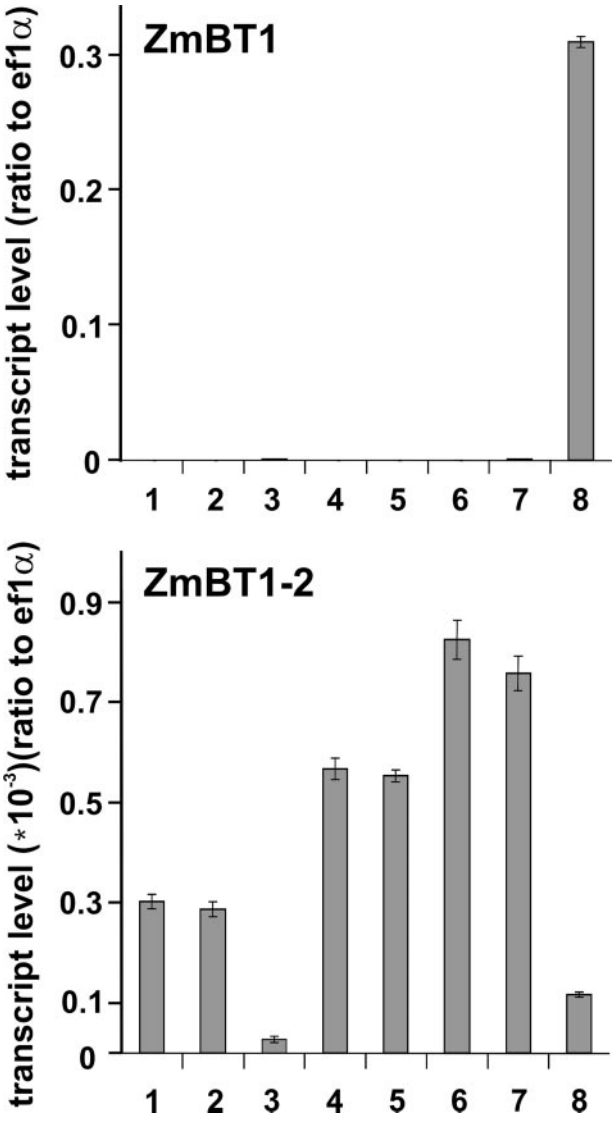

FIGURE 8. **Expression levels of Zm*BT1* and Zm*BT1–2* in different maize tissues.** The transcript levels were determined by quantitative real-time RT-PCR using gene-specific primers. The elongation factor 1α (*EF-1*α) was selected as a housekeeping gene from *Z. mays* (NCBI accession number AF136829, internal control). The relative transcript levels of Zm*BT1* and Zm*BT1–2* were shown as the ratio to the maize EF-1α. 100 ng of total RNA from maize tissues were assayed in triplicates. Data are the mean ± S.E. of four independent experiments. *Lane 1*, leaf; *lane 2*, stem; *lane 3*, root; *lane 4*, young tassel; *lane 5*, mature tassel; *lane 6*, silk; *lane 7*, endosperm (6 days after pollination); *lane 8*, endosperm (15 days after pollination).

should possess at least a second BT1 isoform. Indeed, Southern blot analyses revealed that the maize genome carries two distinct *BT1* homologues (Fig. 3) and the second maize BT1 homologue (ZmBT1–2) was recently identified as well. Furthermore, the analysis of the rice genome revealed even three different *BT1* homologues (35).

Interestingly, the phylogenetic analyses exhibit a subdivision of the BT1 protein family into two biochemically distinct groups (Fig. 2): the first group comprises BT1 homologues restricted to cereals where they are supposed to mediate the ADP-Glc transport into cereal endosperm storage plastids during starch synthesis (14, 34) (Fig. 5; Table 1). The second group of BT1 homologues is present in mono- and dicotyledonous plants. These BT1 homologues are most probably involved in the export of adenine nucleotides synthesized *de novo* inside plastids (15, 16). The phylogenetic classification of the BT1 family into two subgroups (Fig. 2) is further supported by the functional analyses of OsBT1–2 and OsBT1–3, which are identified as adenine nucleotide transporters that are unable to transport ADP-Glc (supplementary materials Table S1). The recently identified ZmBT1–2 homologue clearly belongs to the group of AMP/ADP/ATP carriers. The bootstrap value for the branch that contains OsBT1–3 and ZmBT1–2 is almost maximal (97/100) giving strong support for the notion that ZmBT1–2 is orthologous to an AMP/ADP/ATP carrier. However, the exact position of these two sequences relative to the other AMP/ADP/ATP carriers and the ADP-glucose carrier group is not well resolved (65/100). Nevertheless, based on the phylogeny and the functional information about the proteins, a single separation of the BT1 proteins into a monophyletic group of AMP/ADP/ATP carriers and a monophyletic group of ADP-glucose carriers appears the most parsimonious and therefore most likely scenario. Given the phylogenetic location of these carriers close to the deoxynucleotide carrier group, it is likely that the ancestor of the BT1 group was a nucleotide carrier rather than an ADP-glucose carrier (Fig. 2).

The biochemical classification of the maize *BT1* homologues into two subgroups (Fig. 2) is also supported by the expression analysis. The Zm*BT1* ADP-Glc carrier is exclusively expressed in endosperm tissues during starch synthesis, whereas Zm*BT1–2* shows a ubiquitous expression pattern in hetero- and autotrophic maize tissues as well, with the highest expression levels in silk and tassel (Fig. 8). The ubiquitous expression of Zm*BT1–2* is in line with the proposed function of the recently identified plastidic adenine nucleotide uniporter (St*BT1*), which is supposed to have the general task to provide the cell with adenine nucleotides exclusively synthesized inside plastids (15). Similar observations were made for the expression patterns of the three *BT1* homologues identified in the rice genome. In contrast to the endosperm-specific expression of the BT1 orthologue Os*BT1–1*, both *BT1* paralogues (Os*BT1–2* and Os*BT1–3*) exhibit a wide expression pattern comprising hetero- and autotrophic rice tissues, with the lowest expression level in seeds and roots (35).

Acknowledgments—We thank Sandra Zimmermann for help with the nucleotide uptake experiments. We gratefully acknowledge critical reading of the manuscript by Dipl. Ing. Zeina Tjaden. The ZmBT1-specific antibody was kindly provided by Dr. Thomas D. Sullivan (University of Wisconsin, Madison, WI).

REFERENCES

1. Balmer, Y., Vensel, W. H., Cai, N., Manieri, W., Schurmann, P., Hurkman, W. J., and Buchanan, B. B. (2006) *Proc. Natl. Acad. Sci. U. S. A.* **103,** 2988–2993
2. James, M. G., Denyer, K., and Myers, A. M. (2003) *Curr. Opin. Plant Biol.* **6,** 215–222
3. Nelson, O. E., and Rines, H. W. (1962) *Biochem. Biophys. Res. Commun.* **9,** 297–300
4. Tsai, C. Y., and Nelson, O. E. (1966) *Science* **151,** 341–343
5. Preiss, J., Danner, S., Summers, P. S., Morell, M., Barton, C. R., Yang, L., and Nieder, M. (1990) *Plant Physiol.* **92,** 881–885
6. Bhave, M. R., Lawrence, S., Barton, C., and Hannah, L. C. (1990) *Plant Cell*

2, 581–588
7. Mangelsdorf, P. C. (1926) *Conn. Agric. Exp. Stn. Bull.* **279,** 509–614
8. Wentz, J. B. (1926) *J. Hered.* **17,** 327–329
9. Cao, H., Sullivan, T. D., Boyer, C. D., and Shannon, J. C. (1995) *Physiol. Plant* **95,** 176–186
10. Sullivan, T. D., and Kaneko, Y. (1995) *Planta* **196,** 477–484
11. Pien, F.-M., and Shannon, J. C. (1996) *Plant Physiol.* **111,** (Suppl.) S100
12. Tobias, R. B., Boyer, C. B., and Shannon, J. (1992) *Plant Physiol.* **99,** 146–152
13. Liu, T.-T. Y., Boyer, C. D., and Shannon, J. C. (1992) *Plant Physiol.* **99,** (Suppl.) S39
14. Shannon, J. C., Pien, F. M., Cao, H., and Liu, K. C. (1998) *Plant Physiol.* **117,** 1235–1252
15. Leroch, M., Kirchberger, S., Haferkamp, I., Wahl, M., Neuhaus, H. E., and Tjaden, J. (2005) *J. Biol. Chem.* **280,** 17992–18000
16. Zrenner, R., Stitt, M., Sonnewald, U., and Boldt, R. (2006) *Annu. Rev. Plant Biol.* **57,** 805–836
17. Tjaden, J., Schwöppe, C., Möhlmann, T., Quick, P. W., and Neuhaus, H. E. (1998) *J. Biol. Chem.* **273,** 9630–9636
18. Haferkamp, I., Hackstein, J. H., Voncken, F. G., Schmit, G., and Tjaden, J. (2002) *Eur. J. Biochem.* **269,** 3172–3181
19. Dellaporta, S. T., Wood, J., and Hicks, J. B. (1983) *Plant Mol. Biol. Rep.* **4,** 19–21
20. Sambrook, J., Fritsch, E. F., and Maniatis, T. (1989) *Molecular Cloning: A Laboratory Manual*, Cold Spring Harbor Laboratory, Cold Spring Harbor, NY
21. Studier, F. W., Rosenberg, A. H., Dunn, J. J., and Dubendorff, J. W. (1990) *Methods Enzymol.* **185,** 60–89
22. Krause, D. C., Winkler, H. H., and Wood, D. O. (1985) *Proc. Natl. Acad. Sci. U. S. A.* **82,** 3015–3019
23. Winkler, H. H. (1986) *Methods Enzymol.* **125,** 253–259
24. Mangold, H. K. (1967) in *Nucleic Acids and Nucleotides* (Stahl, E., ed) pp. 749–769, Springer, Heidelberg, Germany
25. Jeanmougin, F., Thompson, J. D., Gouy, M., Higgins, D. G., and Gibson, T. J. (1998) *Trends Biochem. Sci.* **23,** 403–405
26. Guindon, S., Lethiec, F., Duroux, P., and Gascuel, O. (2005) *Nucleic Acids Res.* **33,** W557–W559
27. Edgar, R. C. (2004) *BMC Bioinformatics* **5,** 113
28. Sullivan, T. D., Strelow, L. I., Illingworth, C. A., Phillips, R. L., and Nelson, O. E., Jr. (1991) *Plant Cell* **3,** 1337–1348
29. Saraste, M., and Walker, J. E. (1982) *FEBS Lett.* **144,** 250–254
30. Millar, A. H., and Heazlewood, J. L. (2003) *Plant Physiol.* **131,** 443–453
31. Tjaden, J., Haferkamp, I., Boxma, B., Tielens, A. G., Huynen, M., and Hackstein, J. H. (2004) *Mol. Microbiol.* **51,** 1439–1446
32. Emanuelsson, O., Nielsen, H., and von Heigne, G. (1999) *Protein Sci.* **8,** 978–984
33. Petsalaki, E. I., Bagos, P. G., Litou, Z. I., and Hamodrakas, S. J. (2006) *Genomics Proteomics Bioinformatics* **4,** 48–55
34. Patron, N. J., Greber, B., Fahy, B. F., Laurie, D. A., Parker, M. L., and Denyer, K. (2004) *Plant Physiol.* **135,** 2088–2097
35. Toyota, K., Tamura, M., Ohdan, T., and Nakamura, Y. (2006) *Planta* **223,** 248–257
36. The Arabidopsis Genome Initiative (2000) *Nature* **408,** 796–815
37. Möhlmann, T., Tjaden, J., Henrichs, G., Quick, W. P., Häusler, R., and Neuhaus, H. E. (1997) *Biochem. J.* **324,** 503–509
38. Haferkamp, I., Schmitz-Esser, S., Linka, N., Urbany, C., Collingro, A., Wagner, M., Horn, M., and Neuhaus, H. E. (2004) *Nature* **432,** 622–625
39. Heimpel, S., Basset, G., Odoy, S., and Klingenberg, M. (2001) *J. Biol. Chem.* **276,** 11499–11506
40. Klingenberg, M. (1979) *Methods Enzymol.* **56,** 245–252
41. Stubbs, M. (1981) *Int. Encycl. Pharm. Ther.* **107,** 283–304
42. Flügge, U. I. (1992) *Biochim. Biophys. Acta* **1110,** 112–118
43. Amores, M. V., Hortelano, P., Garcia-Salguero, L., and Lupianez, J. A. (1994) *Mol. Cell. Biochem.* **137,** 117–125
44. Wenderoth, I., Scheibe, R., and von Schaewen, A. (1997) *J. Biol. Chem.* **272,** 26985–26990
45. Prinz, W. A., Aslund, F., Holmgren, A., and Beckwith, J. (1997) *J. Biol. Chem.* **272,** 15661–15667
46. Sancenon, V., Puig, S., Mateu-Andres, I., Dorcey, E., Thiele, D. J., and Penarrubia, L. (2004) *J. Biol. Chem.* **279,** 15348–15355
47. Vandesompele, J., De Preter, K., Pattyn, F., Poppe, B., Van, R. N., De Paepe, A., and Speleman, F. (2002) *Genome Biol.* **3,** RESEARCH0034
48. Dean, J. D., Goodwin, P. H., and Hsiang, T. (2002) *Plant Mol. Biol. Rep.* **20,** 347–356
49. Mahe, A., Grisvard, J., and Dron, M. (1992) *Mol. Plant-Microbe Interact.* **5,** 242–248
50. Sturzenbaum, S. R., and Kille, P. (2001) *Comp. Biochem. Physiol. B Biochem. Mol. Biol.* **130,** 281–289
51. Denyer, K., Dunlap, F., Thorbjørnsen, T., Keeling, P., and Smith, A. E. (1996) *Plant Physiol.* **112,** 779–785
52. Beckles, D. M., Smith, A. M., and ap Rees, T. (2001) *Plant Physiol.* **125,** 818–827
53. Bowsher, C. G., Scrase-Field, E. F., Esposito, S., Emes, M. J., and Tetlow, I. J. (2007) *J. Exp. Bot.* **58,** 1321–1332
54. Shannon, J. C., Pien, F.-M., and Liu, K. C. (1996) *Plant Physiol.* **110,** 835–843
55. Kruger, N. J., and von Schaewen, A. (2003) *Curr. Opin. Plant Biol.* **6,** 236–246
56. Neuhaus, H. E., Henrichs, G., and Scheibe, R. (1993) *Plant Physiol.* **101,** 573–578
57. Kammerer, B., Fischer, K., Hilpert, B., Schubert, S., Gutensohn, M., Weber, A., and Flügge, U. I. (1998) *Plant Cell* **10,** 105–117
58. Tjaden, J., Möhlmann, T., Kampfenkel, K., Henrichs, G., and Neuhaus, H. E. (1998) *Plant J.* **16,** 531–540